

## ORIGINAL ARTICLE

# Plasma extracellular vesicle microRNA-491-5p as diagnostic and prognostic marker for head and neck squamous cell carcinoma

Wittaya Panvongsa<sup>1,2</sup> | Teerada Siripoon<sup>3</sup> | Wittawin Worakitchanon<sup>2,4</sup> | Lalida Arsa<sup>5</sup> | Narumol Trachu<sup>6</sup> | Natini Jinawath<sup>7,8</sup> | Nuttapon Ngamphaiboon<sup>2,3</sup> | Arthit Chairoungdua<sup>1,2,4</sup> 

<sup>1</sup>Toxicology Graduate Program, Faculty of Science, Mahidol University, Bangkok, Thailand

<sup>2</sup>Excellent Center for Drug Discovery (ECDD), Mahidol University, Bangkok, Thailand

<sup>3</sup>Division of Medical Oncology, Department of Medicine, Faculty of Medicine Ramathibodi Hospital, Mahidol University, Bangkok, Thailand

<sup>4</sup>Department of Physiology, Faculty of Science, Mahidol University, Bangkok, Thailand

<sup>5</sup>Molecular Histopathology Laboratory, Department of Pathology, Faculty of Medicine Ramathibodi Hospital, Mahidol University, Bangkok, Thailand

<sup>6</sup>Research Center, Faculty of Medicine Ramathibodi Hospital, Mahidol University, Bangkok, Thailand

<sup>7</sup>Program in Translational Medicine, Faculty of Medicine Ramathibodi Hospital, Mahidol University, Bangkok, Thailand

<sup>8</sup>Integrative Computational BioScience Center (ICBS), Mahidol University, Nakhon Pathom, Thailand

## Correspondence

Nuttapon Ngamphaiboon, Medical Oncology, Department of Medicine, Faculty of Medicine Ramathibodi Hospital, Mahidol University, 270 Rama 6 Road, Ratchathewi, Bangkok 10400, Thailand.  
Email: nuttapon.nga@mahidol.ac.th

Arthit Chairoungdua, Department of Physiology, Faculty of Science, Mahidol University, 272 Rama 6 Road, Ratchathewi, Bangkok 10400, Thailand.  
Email: arthit.chi@mahidol.ac.th

## Funding information

Mahidol University and Thailand Science Research and Innovation (Thailand Research Fund), Grant/Award Number: RSA6280043, PHD/0098/2559; National Research Council of Thailand (NRCT), Grant/Award Number: #3484 Project #6908; Thailand Grand Challenge Program for Research University Network (RUN).

## Abstract

Poor survival of patients with locally advanced head and neck squamous cell carcinoma (LA-HNSCC) is partly due to early diagnosis difficulties and the lack of reliable biomarkers for predicting treatment outcomes. In the discovery cohort, plasma-derived extracellular vesicles (EVs) from LA-HNSCC patients ( $n = 48$ ) and healthy volunteers ( $n = 12$ ) were used for profiling for microRNA (miRNA) expression by NanoString analysis. Ten EV-associated miRNAs were differentially expressed between LA-HNSCC patients and healthy volunteers. Subsequently, the results were validated in the individual discovery and additional cases (HNSCC,  $n = 73$ ; control,  $n = 20$ ) by quantitative RT-PCR. Among 10 EV-miRNAs, four (miR-27b-3p, miR-491-5p, miR-1910-5p, and miR-630) were significantly dysregulated in LA-HNSCC patients ( $n = 73$ ) compared with healthy volunteers ( $n = 20$ ). The miRNA prediction models were developed to discriminate HNSCC patients from healthy volunteers. The model using miR-491-5p was selected as a diagnostic biomarker for LA-HNSCC with a sensitivity and specificity of 46.6% and 100%, respectively ( $P < .001$ ). The dynamic

**Abbreviations:**  $\Delta$ miRNA, dynamic changes in microRNA prediction score; AUC, area under the receiver operating characteristic curve; CT, computed tomography; DFS, disease-free survival; EV, extracellular vesicle; EV-miRNA, extracellular vesicle-associated microRNA; FC, fold change; GO, Gene Ontology; HNSCC, head and neck squamous cell carcinoma; HOTAIR, homeobox transcript antisense RNA; HPV, human papillomavirus; KEGG, Kyoto Encyclopedia of Genes and Genomes; LA-HNSCC, locally advanced head and neck squamous cell carcinoma; miR, microRNA; miRNA, microRNA; NTA, nanoparticle tracking analysis; OPSCC, oropharyngeal squamous cell carcinoma; OS, overall survival; OSCC, oral squamous cell carcinoma; qRT-PCR, quantitative real-time PCR; ROC, receiver operating characteristic; TCGA, The Cancer Genome Atlas; TEM, transmission electron microscopy.

Nuttapon Ngamphaiboon and Arthit Chairoungdua contributed equally to this study.

This is an open access article under the terms of the Creative Commons Attribution-NonCommercial-NoDerivs License, which permits use and distribution in any medium, provided the original work is properly cited, the use is non-commercial and no modifications or adaptations are made.

© 2021 The Authors. *Cancer Science* published by John Wiley & Sons Australia, Ltd on behalf of Japanese Cancer Association.

changes of miRNA model score ( $\Delta$ miRNAs) were determined using scores pre- and postdefinitive treatment to further investigate the prognostic value of miRNA prediction models. The univariate and multivariate analyses indicated that  $\Delta$ miR-491-5p was the most powerful and independent prognostic indicator for overall survival (hazard ratio [HR] 5.66, 95% confidence interval, 1.77-18.01;  $P = .003$ ) and disease-free survival (HR 2.82, 95% CI, 1.13-7.05;  $P = .027$ ) of HNSCC patients. In summary, the miR-491-5p prediction model could serve as a blood-based diagnostic marker for LA-HNSCC. Moreover,  $\Delta$ miR-491-5p could be a potential monitoring prognostic marker to reflect the survival of HNSCC patients.

#### KEYWORDS

biomarker, extracellular vesicle, head and neck squamous cell carcinoma, liquid biopsy, miRNA

## 1 | INTRODUCTION

Head and neck squamous cell carcinoma, an aggressive heterogeneous malignancy arising in the oropharynx, lip, oral cavity, larynx, and hypopharynx, is the seventh most common cancer worldwide.<sup>1,2</sup> The classical risk factors related to the development of HNSCC are smoking and excessive alcohol consumption (approximately 75%) and HPV infection (approximately 25%).<sup>3,4</sup> The prevalence of HPV-positive OPSCC is considerably high, at 60%-70%, especially in the United States and developed countries, compared with less than 10% in low- and middle-income countries.<sup>5-7</sup> Human papillomavirus-positive OPSCC shows a significantly better response to treatment and better OS than HPV-negative OPSCC.<sup>8</sup> Although HPV status and/or p16 expression are well-known prognostic markers for the survival of OPSCC, it contains several limitations for clinical applications.

Two-thirds of patients with HNSCC present with locally advanced stage disease, and 80% of cases involve the regional lymph nodes. Currently, there is no standard recommendation for early detection screening. The 5-year OS of these patients is approximately 40%-60%.<sup>9</sup> Half of the patients with locally advanced disease show tumor recurrence within the first 2 years. Recurrent/metastatic HNSCC patients have a poor prognosis, and the median OS is approximately 1 year.<sup>10</sup> To date, there is no molecular biomarker for patient surveillance that can assist in identifying HNSCC patients that are at high risk for tumor recurrence or progression.<sup>11,12</sup> Thus, identifying an easily accessible and universal diagnostic and prognostic marker for HNSCC remains an essential goal for scientists and clinicians.

MicroRNAs are a family of small noncoding RNAs of 19-22 nucleotides in length that participate in posttranscriptional gene regulation through complementary base pairing with the 3'-UTR of target mRNA and regulate a variety of molecular processes required for normal tissue development and cellular functions.<sup>13</sup> Aberrant expression of miRNAs has been associated with several human diseases, including cancer, suggesting their potential as diagnostic

and prognostic markers.<sup>13,14</sup> Exosomes are small EVs secreted from various cell types with a diameter of 30-150 nm that can carry molecules such as mRNA, miRNA, DNA, lipids, and proteins. Transmission electron microscopy has shown that exosomes have a round or cup-shaped morphology with a density of 1.10-1.21 g/mL in the sucrose gradient.<sup>15,16</sup> Exosomes play roles in cell-cell communication by transporting their cargo between cells.<sup>17</sup> Tumor-derived exosomal miRNAs can induce malignant phenotypes of recipient cells.<sup>18,19</sup> Increasing evidence has suggested that circulating EV-miRNAs could be promising diagnostic, prognostic, and predictive biomarkers in various cancer types.<sup>19,20</sup> However, studies on the expression profiles of circulating EV-miRNAs in HNSCC and their potential as diagnostic and prognostic molecular biomarkers are limited. Here, we identified an EV-associated miRNA as a potential blood-based diagnostic and prognostic biomarker for LA-HNSCC.

## 2 | MATERIALS AND METHODS

### 2.1 | Patient specimens

A prospective multidisciplinary observation study of HNSCC patients treated at Ramathibodi Hospital, Mahidol University has accrued eligible patients since 2016. The study enrolled patients with nonmetastatic HNSCC treated according to the standard of care prospectively. All patients were diagnosed with HNSCC and treated according to the current standard of care at their treating physician's discretion. Data on patient characteristics, treatments, and outcomes were collected prospectively. Blood samples were also obtained from healthy controls who consented to participate in this study. Exclusion criteria for healthy donors included age 18 years or younger, pregnancy, drug addiction, chronic diseases, active infectious diseases, and congenital diseases. The protocol was approved by the Ethics Committee of Ramathibodi Hospital, Mahidol University. Written informed consent was obtained from all subjects.

## 2.2 | Study design

The experimental outline of this study is summarized in Figure 1. Peripheral blood samples of the discovery cohort were taken before definitive treatment (surgery, radiation, or concurrent chemoradiation) and were used for miRNA profiling analysis (12 healthy controls vs 48 HNSCC patients) (NanoString Technology). The differential

expression of miRNAs was further validated using qRT-PCR in the same cohort and additional patients (12 + 8 healthy controls vs 48 + 25 HNSCC patients). After completing definitive treatment, patients were followed according to the standard of care recommendations at the treating physician's discretion (approximately every 3-6 months). Patients lost to follow-up or unavailable posttreatment blood samples were excluded from pre-posttreatment analysis

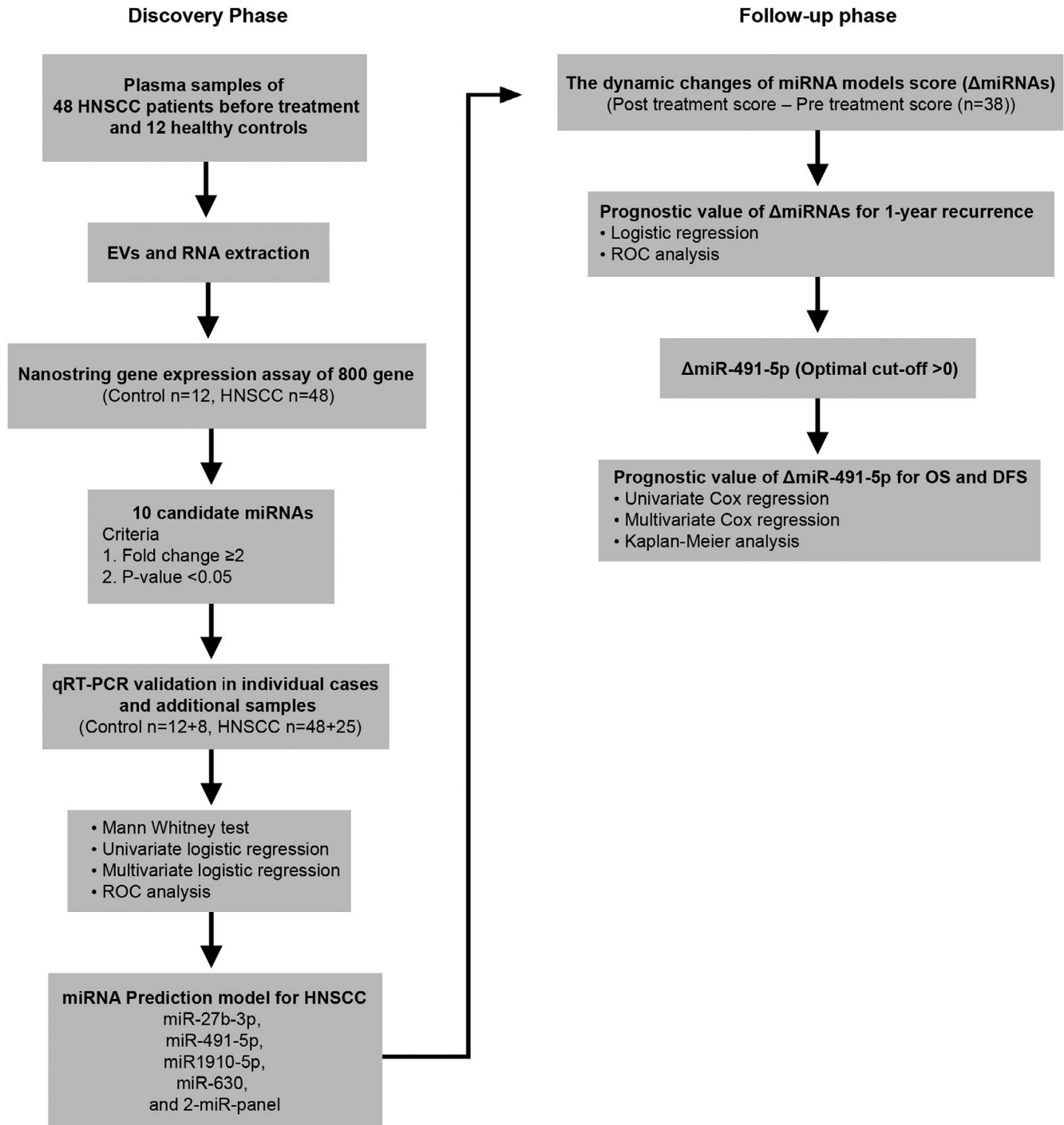


**FIGURE 1** Overview of study design and numbers of participants included in the discovery phase (left) and validation phase (right).  $\Delta$ miRNA, dynamic changes in microRNA prediction score; DFS, disease-free survival; EV, extracellular vesicle; HNSCC, head and neck squamous cell carcinoma; OS, overall survival; qRT-PCR, quantitative real-time PCR; ROC, receiver operating characteristic

( $n = 35$ ). For the remaining patients ( $n = 38$ ) or the follow-up group, posttreatment blood samples were collected at 3 months after completing definitive treatment as the second time point. Recurrence and metastasis of HNSCC were determined based on pathological verification and imaging. The survival of each patient was cross-checked with the National Security Death Index of Thailand.

### 2.3 | Plasma extracellular vesicle isolation

Extracellular vesicles were isolated using the ExoQuick kit (SBI) according to the manufacturer's recommended protocol. Plasma samples were centrifuged at 12 000  $g$  at 4°C for 15 minutes to eliminate cell debris. The ExoQuick reagent was then mixed with 400  $\mu$ L plasma, and samples were incubated at 4°C overnight. The EV fractions were precipitated by centrifugation at 1500  $g$  for 30 minutes. The supernatant was discarded, and samples were subjected to additional centrifugation at 1500  $g$  for 5 minutes to remove the residual solution. The pellet was resuspended in 300  $\mu$ L PBS for subsequent analysis.

### 2.4 | Western blot analysis

Equal amounts of samples were resolved by SDS-PAGE and subsequently transferred to a PVDF membrane (Millipore). Membranes were incubated overnight at 4°C with anti-flotillin-1, anti-TSG101 (Abcam), anti-CD81 (Santa Cruz Biotechnology), and anti-Cyt-C (Cell Signaling Technology) Abs. After washing, membranes were incubated with HRP-conjugated secondary Abs (Jackson ImmunoResearch Laboratories) for 1 hour at room temperature. The signals were detected using the enhanced SuperSignal Luminata Crescendo Western HRP Substrate (Merck Millipore) and exposed onto hyperfilm (Amersham).

### 2.5 | Transmission electron microscopy

Extracellular vesicle samples were mixed with 2% paraformaldehyde, applied onto a Formvar-carbon-coated 300 mesh copper grid (Electron Microscopy Sciences), and dried at room temperature for 20 minutes. The samples were then fixed with 5% glutaraldehyde, washed with distilled water, and stained with 2% uranyl acetate for 1 minute. After washing, the samples were visualized under a TEM (HT7700; Hitachi) at 40 000 $\times$  magnification.

### 2.6 | Nanoparticle tracking analysis

Equal amounts of EV samples were diluted with PBS (less than 100 particles per frame). The size distribution was measured using NanoSight NS300 with a 405 nm laser instrument (NTA version 3; Malvern Instruments) in triplicate for 60 seconds.

### 2.7 | RNA extraction and miRNA expression analysis

Total RNAs were isolated from EVs using the miRNeasy Mini kit (Qiagen) according to the manufacturer's protocol. The quantity of the RNA was determined by measuring A260 / A280 and A260 / A230 ratios using a NanoDrop ND2000 (Thermo Fisher Scientific). The expression levels of miRNAs were determined using the nCounter human miRNA panel version 3 consisting of approximately 800 miRNA targets (NanoString Technologies). Raw data were collected and analyzed using nSolver 4.0 software. All data were normalized using the geometric mean of the top 100 miRNAs and two spike-in miRNAs (cel-miR-248 and cel-miR-254) and presented as FC.

### 2.8 | Quantitative real-time PCR

The miRNAs were reverse transcribed with a miScript Reverse Transcription Kit (Qiagen) according to the manufacturer's instructions. The expressions of miRNAs were measured by qRT-PCR using miScript SYBR Green PCR kits with specific primers (Qiagen). The expression level of each miRNA was normalized by that of small RNA (RNU6) and analyzed using the  $2^{-\Delta\Delta CT}$  method.

### 2.9 | Pathway enrichment analysis

The potential target genes of hsa-miR-491-5p were predicted using the miRSystem database (<http://mirsystem.cgm.ntu.edu.tw/index.php> version 20160513), an integrated system of seven prediction algorithm programs (DIANA, miRanda, miRBridge, PicTar, PITA, rna22, and TargetScan). This database also contains validated data on miRNA-target gene interactions from TarBase and miRecords. Only target genes identified by at least three prediction algorithms were annotated with KEGG pathway and GO analysis by WebGestalt's gene-set enrichment analysis and the miRsystem database, respectively. The adjusted  $P$  value of each enriched pathway was calculated following the method of Benjamini and Hochberg.<sup>21</sup> The statistically enriched pathways were obtained using a hypergeometric test ( $P < .05$ ).

### 2.10 | The Cancer Genome Atlas data acquisition

The expressions of miR-491-5p in 503 HNSCC tissues and 41 normal tissues were analyzed from the TCGA database using the miRNA Target Viewer (miR-TV) (<http://mirtv.ibms.sinica.edu.tw>).<sup>22</sup>

### 2.11 | Statistical analysis

All statistical analyses were calculated and displayed using SPSS PASW Statistics version 18.0 (SPSS Inc.) and GraphPad Prism version

8.0.0 (GraphPad Software). The miRNA expression data were applied to binary logistic regression to undertake individual miRNA prediction models. The miRNA panel model was generated using stepwise multivariate logistic regression analyses. Receiver operating characteristic curves were constructed to assess the diagnostic performances of the miRNA prediction models to discriminate between healthy controls and patients. The optimal cut-off point, sensitivity, and specificity were obtained from the Youden index. As all patients were followed for at least 1 year, we considered 1-year disease recurrence as an end-point to generate the new cut-off score to categorize patients into low- and high-risk groups. We applied the miRNA prediction models to the miRNA expression data of pretreatment and posttreatment samples. The  $\Delta$ miRNAs score was calculated as the posttreatment score minus the pretreatment score. The 1-year recurrence rate was calculated from the time of first diagnosis until 1 year or the date of relapse. Binary logistic regression was used to examine the association between the miRNA models and the 1-year recurrence rate. Univariate Cox analyses were undertaken to observe the correlation between  $\Delta$ miRNAs and clinical parameters with OS and DFS using the log-rank test. We calculated OS from the first day of diagnosis until death or the last follow-up. Disease-free survival was defined as the time from diagnosis to the time of recurrence, death, or the last follow-up. Multivariate Cox analyses were performed to evaluate the hazard ratios and the independent prognostic value of  $\Delta$ miRNAs within the setting of standard clinical parameters. The survival distributions in different groups were tested by the Kaplan-Meier method and the log-rank method. For all statistical analyses, a *P*-value < .05 was considered statistically significant.

### 3 | RESULTS

#### 3.1 | Characteristics of HNSCC patients and healthy controls

The discovery cohort consisted of 48 HNSCC patients and 12 healthy controls. In the qRT-PCR validation cohort, a total of 73 patients with HNSCC and 20 healthy controls were included. The majority of participants were male (80%), with a mean age of  $64 \pm 11$  years old (Table 1). Approximately 76.4% of HNSCC patients were smokers. The major tumor primary sites were oropharynx (30%) and larynx (25%). Most patients presented with locally advanced stage (IVa, 51%; IVb, 29%). Expression of p16 and tumor HPV status were positive in 20.4% and 7.8% of HNSCC patients, respectively. For patients in the follow-up cohort (*n* = 38), the baseline patient characteristics were comparable with those of the overall patient group. The majority of patients in the follow-up cohort received chemoradiotherapy (86.8%) as a definitive treatment. Recurrence and death occurred in 39.5% and 44.7% of patients in the follow-up cohort, respectively. The median DFS and OS were 17.6 and 23 months, respectively.

For the healthy controls, the majority of participants were male (70%), with a mean age of  $51.4 \pm 10$  years old (Table S1). Approximately 60% of healthy controls were nonsmokers.

**TABLE 1** Clinical characteristics of patients with head and neck squamous cell carcinoma (HNSCC)

Variable	HNSCC (overall)	HNSCC (follow-up)
	n (%)	n (%)
<b>Number</b>	<b>73</b>	<b>38</b>
Sex		
Male	58 (80)	34 (89.5)
Female	15 (20)	4 (10.5)
Age (y), mean $\pm$ SD		
<65	40 (55)	23 (60.5)
$\geq$ 65	33 (45)	15 (39.5)
Smoking (pack-years)		
Mean	18.2	23.55
Ever	55 (76.4)	33 (86.8)
Never	17 (23.6)	5 (13.2)
N/A	1	0 (0.0)
Primary site		
Oral cavity	15 (20.5)	4 (10.5)
Oropharynx	22 (30.1)	13 (34.2)
Hypopharynx	14 (19.2)	9 (23.7)
Larynx	18 (24.7)	10 (26.3)
Nasal cavity	1 (1.4)	1 (2.6)
Paranasal sinus	3 (4.1)	1 (2.6)
Clinical stage		
I-II	3 (4.1)	3 (7.9)
III	11 (15.1)	8 (21.1)
Iva	37 (50.7)	20 (52.6)
IVb	21 (28.8)	7 (18.4)
IVc	1 (1.4)	0 (0.0)
T classification <sup>a</sup>		
T1-2	14 (19.2)	10 (26.3)
T3	26 (35.6)	15 (39.5)
T4a/b	33 (45.2)	13 (34.2)
N classification <sup>b</sup>		
N0	15 (20.5)	10 (26.3)
N1	8 (11)	5 (13.2)
N2	40 (54.8)	20 (52.6)
N3	10 (13.7)	3 (7.9)
M classification		
M0	71 (97.3)	37 (97.4)
M1	2 (2.7)	1 (2.6)
p16 status		
Positive	10 (20.4)	4 (11.1)
Negative	39 (79.6)	32 (88.9)
Not tested	24	2
HPV DNA		
Positive	4 (7.8)	2 (6.1)

(Continues)

TABLE 1 (Continued)

Variable	HNSCC (overall)	HNSCC (follow-up)
	n (%)	n (%)
<b>Number</b>	<b>73</b>	<b>38</b>
Negative	47 (92.2)	31 (93.9)
Not tested	22	5
Definitive treatment		
Surgery	11 (15.1)	3 (7.9)
Chemoradiotherapy	57 (78)	34 (86.8)
Radiotherapy	1 (1.4)	1 (2.6)
Lost to follow-up	4 (5.5)	0 (0.0)
Tumor recurrence		
Yes	27 (37)	15 (39.5)
No	46 (63)	23 (60.5)
Death		
Yes	37 (50.7)	17 (44.7)
No	36 (49.3)	21 (55.3)

Abbreviations: HPV, human papillomavirus; N/A, not applicable.

<sup>a</sup>Primary tumor stage.

<sup>b</sup>Regional lymph node stage.

### 3.2 | Extracellular vesicle characterization

The isolated EVs were characterized following recommendations by International Society of Extracellular Vesicles in MISEV2018.<sup>23</sup> The morphology of isolated EVs was examined by TEM. Extracellular vesicles from both healthy controls and HNSCC patients appeared as membrane-bound vesicles with a size of less than 150 nm (Figure 2A). The NTA was applied to confirm the size of the isolated EVs. The average sizes were  $150 \pm 0.21$  and  $145.7 \pm 0.04$  nm for healthy controls and HNSCC patients, respectively (Figure 2B). Samples were further characterized by evaluating the expression of recommended protein markers for EVs. The transmembrane proteins flotillin-1 and CD81 and cytosolic protein TSG101 were detected in all isolated EVs from healthy controls and HNSCC patients (Figure S1). These results indicated that the isolated vesicles were indeed small EVs and suitable for subsequent analysis.

### 3.3 | Dysregulation of miRNAs in plasma-derived EVs of HNSCC patients

To identify the differentially expressed miRNAs in plasma-derived EVs in HNSCC, we undertook miRNA profiling using NanoString analysis, as described in Materials and Methods. As shown by a volcano plot in Figure 2C, the expressions of 10 EV-miRNAs were significantly dysregulated in HNSCC, with a FC  $\geq 2$  and  $P < .05$ . Among the miRNAs, five miRNAs were upregulated (miR-144-3p, miR-1910-5p, miR-491-5p, miR-660-5p, and miR-630) and five miRNAs

were downregulated (miR-1827, miR-342-3p, miR-27b-3p, miR-592, and miR-337-5p) in HNSCC. The list of these 10 miRNAs with FC and  $P$  values is shown in Table S2.

We further validated the expression of the candidate miRNAs from NanoString results in 73 HNSCC patients and 20 healthy controls from the discovery cohort with additional cases using qRT-PCR. The miRNAs with a cycle threshold more than 36 were excluded. After Mann-Whitney and univariate testing, four signature miRNAs (miR-27b-3p, miR-491-5p, miR-1910-5p, and miR-630) were identified as significantly dysregulated in plasma-derived EVs of HNSCC and were selected for subsequent analysis (Figure 2D and Table 2).

### 3.4 | Diagnostic value of signature miRNA prediction models

We compared the miRNA profiles in plasma-derived EVs of healthy controls ( $n = 20$ ) and all patients diagnosed with HNSCC ( $n = 73$ ). The ROC analysis was carried out to assess the diagnostic capacity of the four signature miRNA prediction models to discriminate HNSCC patients from healthy controls. As shown in Table 3 and Figure S2, all signature miRNA models showed significant diagnostic power ( $P < .001$ ) with AUC up to 0.829 with various sensitivities and specificities. To increase the diagnostic efficacy, we combined these four signature miRNAs as a miRNA panel model for HNSCC detection using stepwise multivariate logistic regression (Table 2). The panel with miR-27b-3p and miR-1910-5p, referred to hereafter as the two-miRNA panel, revealed a diagnostic power with an AUC of 0.888 (95% CI, 0.80-0.94;  $P < .001$ ) with a sensitivity and specificity of 79.5% and 95%, respectively (Table 3 and Figure S2).

To determine whether the proposed signature miRNA prediction models were associated with clinical characteristics of HNSCC, the relation between the score of each miRNA prediction model and the clinical stage was examined. According to the Mann-Whitney analysis, only the score of the miR-491-5p model was significantly correlated with the clinical stage, with a  $P$  value of .0077 (Figure S3A). We also examined the correlation between the score of each of the miRNA prediction models with other clinical characteristics. As shown in Figure S3, no significant correlation was observed between the score of miRNA prediction models with sex, smoking status, p16 status, or primary tumor site; only the score of the miR-27b-3p model was associated with patient age more than 65 years ( $P = .0433$ ).

### 3.5 | Prognostic value of miRNA prediction models for HNSCC

To determine the ability of the five miRNA prediction models as monitoring tools to predict the treatment outcome of HNSCC patients, the dynamic change of miRNA prediction scores ( $\Delta$ miRNAs; the posttreatment score minus the pretreatment score) was

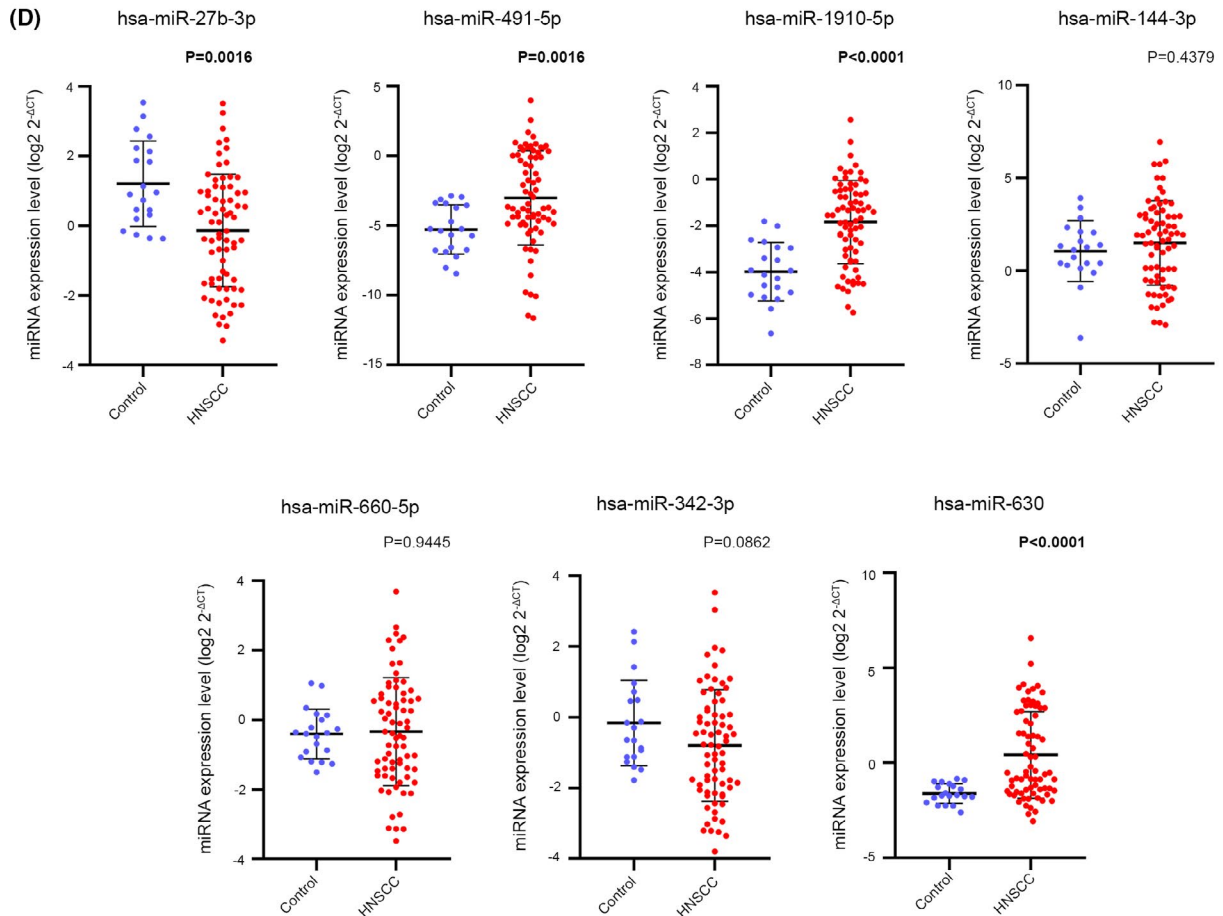
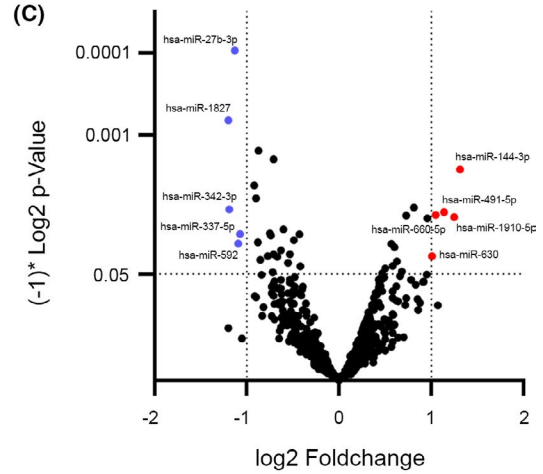
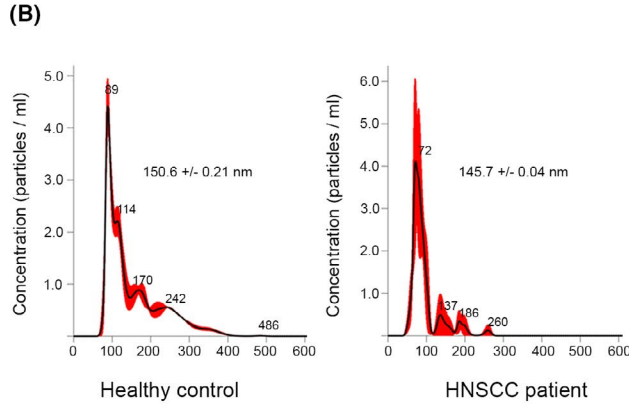
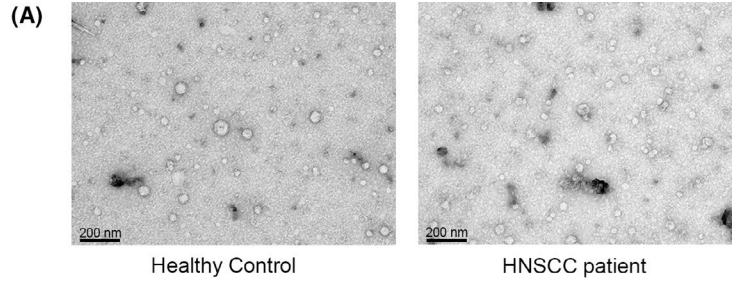


**FIGURE 2** MicroRNA (miRNA) expression profile in plasma-derived extracellular vesicles (EVs) of healthy controls and head and neck squamous cell carcinoma (HNSCC) patients. A, Transmission electron microscopy images of EVs from plasma of healthy controls and HNSCC patients. Scale bar = 200 nm. B, Size distribution by nanoparticle tracking analysis. The average size of EVs was calculated from three independent injections. C, Volcano plot representing the relationship between  $\log_2$  fold change (FC) of miRNA expression between EVs of healthy controls and HNSCC patients. Blue and red dots represent downregulated and upregulated miRNAs with FC > 2 and  $P < .05$  in HNSCC, respectively. D, Expression of candidate miRNAs in healthy controls and HNSCC patients was determined by quantitative real-time PCR. Expression of miRNAs was normalized with the expression of RNU6 and represented as scatter plots with  $\log_2(2^{-\Delta\text{CT}})$ . The expression levels of miRNAs between healthy controls ( $n = 20$ ) and HNSCC ( $n = 73$ ) patients were compared by Mann-Whitney test

**TABLE 2** Univariate and multivariate logistic regression of signature microRNAs (miRNAs) in head and neck squamous cell carcinoma

Univariate logistic regression			Multivariate logistic regression (stepwise with four miRNAs)		
miRNAs	Odd ratio (95% CI)	P value	miRNAs	Odd ratio (95% CI)	P value
hsa-miR-27b-3p	0.5521 (0.37-0.80)	.0022	hsa-miR-27b-3p	0.5051 (0.32-0.8)	.0035
hsa-miR-491-5p	1.2621 (1.06-1.49)	.0081	hsa-miR-1910-5p	2.3096 (1.48-3.6)	.0002
hsa-miR-1910-5p	2.1948 (1.48-3.25)	.0001			
hsa-miR-144-3p	1.1017 (0.87-1.39)	.4150			
hsa-miR-660-5p	1.0370 (0.72-1.47)	.8404			
hsa-miR-342-3p	0.7578 (0.54-1.05)	.1007			
hsa-miR-630	2.5536 (1.36-4.78)	.0035			

Abbreviation: CI, confidence interval.

examined. As shown in Table 4 and Figure S4, only  $\Delta\text{miR-491-5p}$  was significantly associated with 1-year recurrence. The cut-off score of  $\Delta\text{miR-491-5p}$  separated low-risk (score  $\leq 0$ ) and high-risk (score  $> 0$ ) patients with 80% sensitivity and 69.23% specificity. Based on this cut-off score, we used Kaplan-Meier survival analysis to examine the prognostic power of  $\Delta\text{miR-491-5p}$ . As shown in Figure 3A,B,  $\Delta\text{miR-491-5p}$  was significantly associated with OS and DFS. The 3-year OS rate was 67.2% among patients in the low-risk group and 14.3% among those in the high-risk group ( $P = .0003$ ). The DFS rate at 3 years was 56% and 22.1% in patients in low-risk and high-risk groups, respectively ( $P = .0017$ ). Disease-free survival and OS of other clinical parameters, including stage, nodal status, and p16 expression, are shown in Figure 3C-H.

Univariate Cox logistic regression analysis revealed that  $\Delta\text{miR-491-5p}$  was significantly associated with patient OS (HR 4.69, 95% CI, 1.60-13.68;  $P = .004$ ) and DFS (HR 3.09; 95% CI, 1.26-7.55;  $P = .013$ ) (Table 5). Multivariate analysis indicated that only  $\Delta\text{miR-491-5p}$  was significantly associated with OS (HR 5.66; 95% CI, 1.77-18.01;  $P = .003$ ) and DFS (HR 2.82; 95% CI, 1.13-7.05;  $P = .027$ ) (Table 6).

### 3.6 | Target genes of miR-491-5p are significantly associated with cancer-related signaling pathways

To understand the biological functions of miR-491-5p, the miRSystem database was used to predict the potential target genes of miR-491-5p and the target genes were analyzed by KEGG pathway and

GO analyses. A total of 224 target genes were predicted to be regulated by miR-491-5p (Table S3). These putative targets were significantly enriched in six KEGG signaling pathways ( $P < .05$ ) (Table S4): axon guidance, microRNAs in cancer, regulation of actin cytoskeleton, taste transduction, C-type lectin receptor signaling pathway, and hepatocellular carcinoma. Interestingly, the predicted target genes of miR-491-5p tended to be associated with several other cancer-related signaling pathways, such as the calcium signaling pathway, transforming growth factor- $\beta$  signaling pathway, and Wnt signaling pathway, although they do not meet statistically significant power. The target genes of miR-491-5p were significantly related to three GO biological process terms, including chromatin binding, enzyme activator activity, and transcription repressor activity ( $P < .05$ ) (Table S5). These results indicate that miR-491-5p regulates several cellular processes that might be involved with the development of HNSCC.

## 4 | DISCUSSION

To the best of our knowledge, this is the first study to evaluate the clinical application of miRNAs in plasma-derived EVs as both diagnostic and prognostic biomarkers in HNSCC. Our study demonstrates two important clinical findings. First, we identified miR-491-5p in plasma-derived EVs as a potential diagnostic marker model for HNSCC patients. Second, the dynamic change of the miR-491-5p prediction score ( $\Delta\text{miR-491-5p}$ ), calculated using scores before and after definitive treatment, represented a strong and independent prognostic factor for OS and DFS in patients with HNSCC.

TABLE 3 Diagnostic value of the five microRNA (miRNA) prediction models in head and neck squamous cell carcinoma

miRNA	Optimal cut-off point	Sensitivity (%)	Specificity (%)	AUC (95% CI)	P value	Diagnostic models
hsa-miR-27b-3p	>86	43.8	100	0.725 (0.62-0.81)	<.001	miR27b-3p-score = $-0.59397 * \text{miR27b-3p} + 1.62739$
hsa-miR-491-5p	>83	46.6	100	0.727 (0.62-0.81)	<.001	miR491-5p-score = $0.2328 * \text{miR491} + 2.25555$
hsa-miR-1910-5p	>83	67.1	90	0.829 (0.73-0.90)	<.001	miR1910-5p-score = $0.78607 * \text{miR1910} + 3.63685$
hsa-miR-630	>79	61.6	95	0.790 (0.70-0.87)	<.001	miR-630-score = $0.9375 * \text{miR630} + 6.85766$
Two-miRNA panel (miR-27b-3p and miR-1910-5p)	>78	79.5	95	0.888 (0.80-0.94)	<.001	Two-miR-score = $0.83708 * \text{miR1910} + (-0.68295 * \text{miR27b}) + 4.26134$

Abbreviations: AUC, area under the receiver operating characteristic curve; CI, confidence interval.

Several studies have focused on the development of blood-based biomarkers for the diagnosis and prognosis of HNSCC; however, these markers have not yet been validated. Elevated nuclear factor- $\kappa$ B-p50 protein in serum ( $\geq 21.85$  ng/ $\mu$ L) by label-free real-time surface plasmon resonance technology significantly separated HNSCC patients (oral cavity, oropharynx, larynx, and nasopharynx cancers) from control cases with a sensitivity and specificity of 87.20% and 87.50%, respectively.<sup>24</sup> Scavenger receptor class A member 5 (scara5) protein was found to be downregulated in the serum of OSCC patients and could differentiate OSCC patients from healthy individuals with 100% sensitivity and 68.4% specificity.<sup>25</sup> Recently, HPV16-L1 DRH1 epitope-specific serum Abs, rather than lifetime exposure to HPV, were linked to HPV16-induced malignant disease. Serum DRH1 Abs showed a 95% sensitivity for HPV16-driven OPSCC, and the diagnostic specificity was 99.46% for men and 95.6% for women.<sup>26</sup> However, this test was limited to patients with HPV-related HNSCC.

Our findings show that five miRNA models could discriminate between HNSCC patients and healthy controls with significant diagnostic power. However, only the miR-491-5p model score was significantly associated with the clinical stage, suggesting the potential role of miR-491-5p in HNSCC development. In contrast, the other miRNAs might be correlated with the host microenvironment and patient baseline characteristics more than the disease. Hence, we selected the miR-491-5p prediction model as a diagnostic tool for HNSCC patients. The miR-491-5p prediction model has a very high specificity rate (100%) in terms of diagnosis. However, the sensitivity was lower (46.6%) compared with the other models evaluated in our study. In fact, other blood-based biomarkers with low sensitivity but high specificity have been suggested as acceptable for clinical practice. For instance,  $\alpha$ -fetoprotein is recommended for diagnosis as a standard of care combined with CT scan or MRI findings in patients with hepatocellular carcinoma, with low sensitivity of 60% and high specificity of 80%.<sup>27</sup> Therefore, we suggest that the miR-491-5p diagnostic model should be evaluated in combination with other techniques such as physical examination and imaging studies (CT, MRI, and PET scans) in the future to explore its use in diagnosis or screening high-risk patients with suspicious HNSCC for whom tissue diagnosis is not possible.

Although several studies have investigated prognostic markers from the blood for HNSCC, no blood-based prognostic marker is currently recommended in clinical practice. To date, only a few studies have investigated the diagnostic and prognostic value of small EV-associated miRNAs in HNSCC patients. The serum-derived exosomal miR-21 and HOTAIR were associated with clinical characteristics of laryngeal squamous cell carcinoma and the combination of miR-21 and HOTAIR discriminated malignant from benign laryngeal disease with a sensitivity of 94.2% and specificity of 73.5%.<sup>28</sup> Hypoxic conditions increased miR-21 levels in OSCC serum-derived exosomes, which was associated with T stage and lymph node metastasis.<sup>29</sup> Saliva-derived exosomal miR-512-3p and miR-412-3p were upregulated in OSCC in a study of 21 OSCC patients and 11 volunteers; ROC analysis showed high AUC values (0.847 and 0.871,

**TABLE 4** Prognostic value for 1-year recurrence of head and neck squamous cell carcinoma of dynamic changes in microRNA prediction scores ( $\Delta$ miRNAs) in pretreatment and posttreatment

Univariate logistic regression			Prognostic value for 1-y recurrence			
miRNAs	Odd ratio (95% CI)	P value	Optimal cut-off point	Sensitivity (%)	Specificity (%)	AUC (95% CI)
$\Delta$ miR-27b-3p	0.98 (0.96-1.00)	.34	$\leq -33$	20	100	0.552 (0.38-0.72)
$\Delta$ miR-491-5p	1.41 (1.02-1.93)	.03	$>0$	80	69.23	0.777 (0.61-0.90)
$\Delta$ miR-1910-5p	1.10 (0.96-1.20)	.19	$>2$	40	84.62	0.635 (0.46-0.79)
$\Delta$ miR-630	1.05 (0.88-1.25)	.59	$>0$	70	80.77	0.742 (0.58-0.88)
$\Delta$ 2-miR-panel (miR-27b-3p and miR-1910-5p)	0.99 (0.96-1.00)	.93	$\leq 10$	70	15.38	0.508 (0.34-0.68)

Abbreviations: AUC, area under the receiver operating characteristic curve; CI, confidence interval.

respectively).<sup>30</sup> In a recent study, increased plasma exosomal miR-196a level was associated with drug sensitivity and poor OS in head and neck cancer patients (HR 2.248). Plasma exosomal miR-196a was able to separate patients in the chemoresistant and chemosensitive groups with a sensitivity of 85% and specificity of 70%.<sup>31</sup> However, the main limitation in using these small EV-miRNAs as a biomarker is that the blood circulation also contains robust levels of endogenous EVs, which suggests the restriction to identify the tumor-specific EV-miRNAs. Additionally, the level of miRNAs in the circulating EVs generally fluctuates between individuals, which strongly indicates the existence of interindividual differences in EV-miRNA levels. To minimize these limitations, we used paired plasma samples to allow for self-normalization of miRNAs in plasma-derived EVs. In our study, paired plasma samples were collected after primary treatment for 3 months and used as a secondary time point, which was the most accurate assessment for treatment response in HNSCC.<sup>32</sup>

MicroRNA-491-5p has been reported as a tumor suppressor in cancer. Overexpression of miR-491-5p in pancreatic cancer cell lines inhibited *Bcl-xL* and *TP53* gene expression and induced cell apoptosis.<sup>33</sup> In glioblastoma, miR-491-5p suppressed glioma cell invasion by targeting MMP-9.<sup>34</sup> Xiao and colleagues recently reported that miR-491-5p functions as a tumor suppressor in colorectal cancer cell lines by inhibiting cell migration, invasion, and proliferation and inducing cell apoptosis.<sup>35</sup> Several functional roles of miR-491-5p have been reported in HNSCC. Huang et al identified miR-491-5p as a metastatic suppressor by targeting the G-protein-coupled receptor kinase-interacting protein 1 (*GIT1*) gene and the low level of miR-491-5p was associated with poor survival of OSCC patients.<sup>36</sup> However, the expression and biological roles of exosomal miR-491-5p in HNSCC are limited. From the TCGA database, we found that the expression of miR-491-5p was significantly downregulated in HNSCC tissue compared with the normal adjacent tissues (Figure S5). This result indicates the inverse correlation between the cellular and circulating levels of EV-miR-491-5p. Several studies proposed that tumor cells use small EVs as a vehicle to get rid of tumor suppressor miRNAs to

maintain or protect their oncogenesis status. For example, expression of the tumor suppressor miR-1246 is downregulated in prostate cancer tissues and cell lines compared with normal samples and is selectively released into exosomes.<sup>37</sup> Bladder cancer cells discard the tumor suppressor miR-23b that restrains metastatic progression via exosomes, leading to its low cellular levels.<sup>38</sup> Therefore, our data suggest that HNSCC cells might release the tumor suppressor miR-491-5p into the circulation through the small EVs in order to maintain their oncogenic status.

The strength of our study is that clinical data and samples were obtained prospectively, which allows for the assessment of patient characteristics, treatments, disease progression, survival, and removal of recall bias data.<sup>39</sup> The miRNA profiles were identified from plasma-derived EVs of patients with different primary tumor sites, which assists us in identifying a universal biomarker for patients with HNSCC. We undertook self-normalization to eliminate the interindividual differences and minimize robust background miRNAs. This method was essential for the precise prediction of posttreatment outcomes. In addition, we found that the miR-491-5p model could potentially be used both as a noninvasive diagnostic and prognostic marker in patients with HNSCC. However, there are some limitations to our study. The observational study resulted from a limited sample size and follow-up time. All patients who participated in this study were from a single center. In addition, various postoperative treatments of this cohort were varied, although most patients (86.8%) received adjuvant chemoradiotherapy. Moreover, the incidence of HPV-associated HNSCC in our study was low (7.8%) compared with patients from Europe and North America.<sup>40</sup> Indeed, low incidences of HPV-associated HNSCC in the Thai population have been previously reported.<sup>41,42</sup> Therefore, further validation in a larger sample size, with long follow-up time, and multicenter studies are warranted.

In conclusion, we developed a miR-491-5p prediction model as a blood-based biomarker for diagnosis in HNSCC. Importantly, we

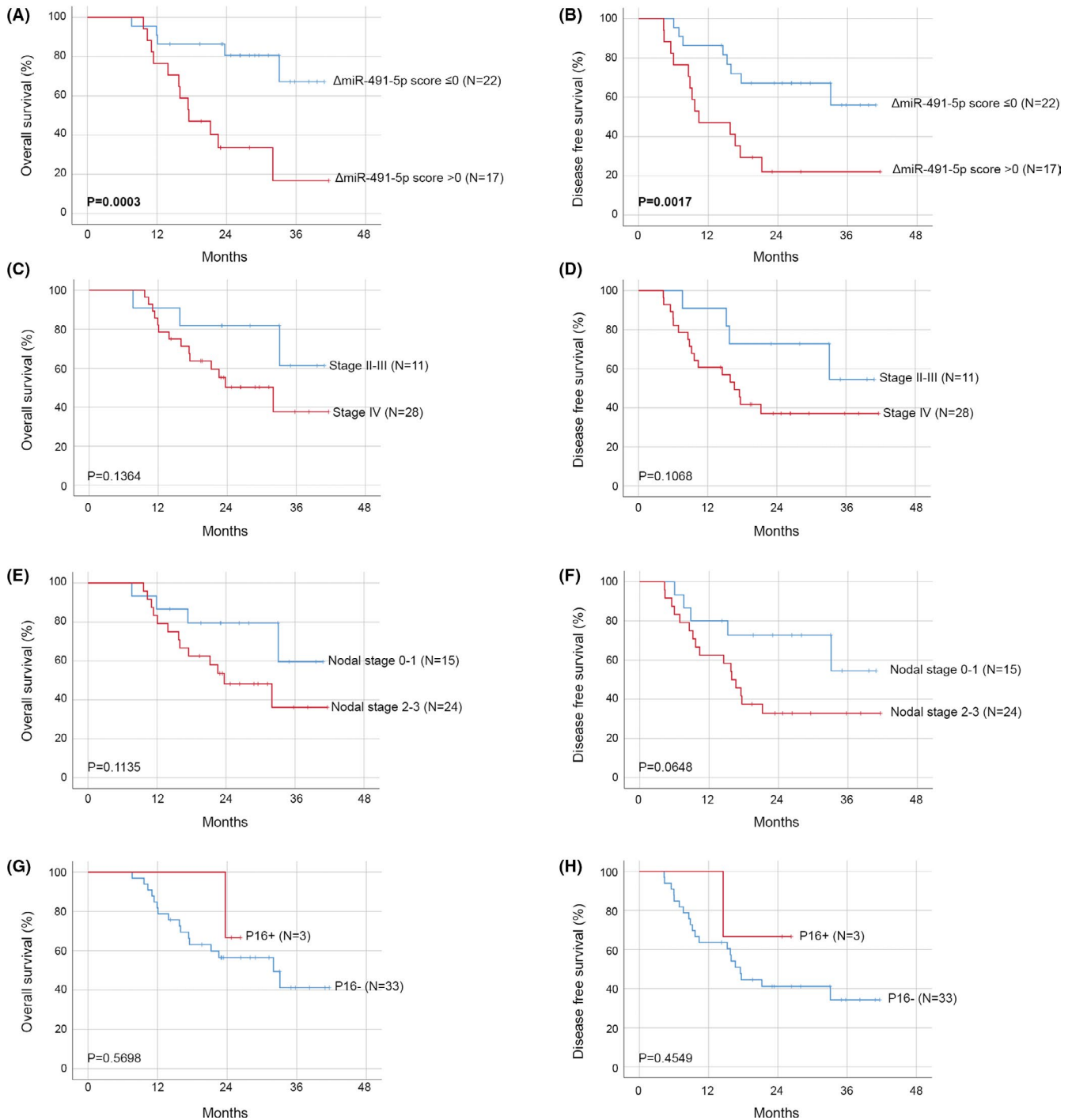


**FIGURE 3** Kaplan–Meier curve and log-rank test of overall survival and disease-free survival in patients with head and neck squamous cell carcinoma according to clinical stage, N stage, p16 status, and dynamic changes in microRNA-491-5p ( $\Delta$ miR-491-5p). A, C, E, G, Overall survival according to clinical stage, N stage, p16 status, and  $\Delta$ miR-491-5p, respectively. B, D, F, H, Disease-free survival according to clinical stage, N stage, p16 status, and  $\Delta$ miR-491-5p, respectively

determined that the dynamic changes of the miR-491-5p prediction score ( $\Delta$ miR-491-5p) from pretreatment and posttreatment might be a potential prognostic biomarker for HNSCC, which could help identify HNSCC patients who will eventually show tumor recurrence. Furthermore, these results could represent an essential step to improve the OS of patients with HNSCC.

#### ACKNOWLEDGMENTS

This project was supported by Mahidol University and Thailand Science Research and Innovation (Thailand Research Fund) (RSA6280043 to AC), the National Research Council of Thailand (NRCT) through the Government Research Grant #3484 (Project #6908 to NN), and the Thailand Grand Challenge Program for

Variable	Hazard ratio for OS (95% CI)	P value	Hazard ratio for DFS (95% CI)	P value
Age ≥65 y vs <65 y	1.39 (0.52-3.69)	.502	1.10 (0.46-2.64)	.825
Overall stage IV vs II-III	2.65 (0.75-9.36)	.131	2.54 (0.85-7.61)	.095
Node 2-3 vs 0-1	2.54 (0.82-7.83)	.104	2.67 (0.97-7.32)	.056
T stage 3-4 vs 1-2	1.00 (0.32-3.07)	.997	1.48 (0.49-4.42)	.476
Non-oro-pharynx vs oro-pharynx	0.48 (0.18-1.25)	.136	0.74 (0.30-1.80)	.516
p16 positive vs negative	0.56 (0.07-4.31)	.581	0.45 (0.06-3.39)	.440
ΔmiR-491-5p score >0 vs ≤0	4.69 (1.60-13.68)	.004	3.09 (1.26-7.55)	.013

Abbreviation: CI, confidence interval.

Variable	Hazard ratio for OS (95% CI)	P value	Hazard ratio for DFS (95% CI)	P value
Age ≥65 vs <65 y	3.47 (0.89-13.56)	.074	2.45 (0.69-8.72)	.165
Overall stage IV vs II-III	3.52 (0.74-16.81)	.113	3.76 (0.89-15.77)	.070
Non-oro-pharynx vs oro-pharynx	0.65 (0.18-2.33)	.507	1.12 (0.34-3.67)	1.125
ΔmiR-491-5p score >0 vs ≤0	5.66 (1.77-18.01)	.003	2.82 (1.13-7.05)	.027

Abbreviation: CI, confidence interval.

**TABLE 5** Univariate Cox regression analysis to evaluate the prognostic factor ΔmiR-491-5p (dynamic changes in microRNA-491-5p prediction score) for overall survival (OS) and disease-free survival (DFS) in patients with head and neck squamous cell carcinoma

**TABLE 6** Multivariate Cox analysis to evaluate ΔmiR-491-5p (dynamic changes in microRNA-491-5p prediction score) as independent prognostic factors for overall survival (OS) and disease-free survival (DFS) in patients with head and neck squamous cell carcinoma

Research University Network (RUN) under the Precision Medicine for Cancer project (to NN). WP was supported by Thailand Science Research and Innovation (Thailand Research Fund) through the Royal Golden Jubilee PhD Program and Mahidol University (PHD/0098/2559).

## DISCLOSURE

The authors have no conflict of interest.

## DATA AVAILABILITY STATEMENT

The authors confirm that the data supporting the findings of this study are available within the article.

## ORCID

Arthit Chairoungdua  <https://orcid.org/0000-0002-0965-126X>

## REFERENCES

- Bray F, Ferlay J, Soerjomataram I, Siegel RL, Torre LA, Jemal A. Global cancer statistics 2018: GLOBOCAN estimates of incidence and mortality worldwide for 36 cancers in 185 countries. *CA Cancer J Clin*. 2018;68:394-424.
- Tangjaturonrasme N, Vatanasapt P, Bychkov A. Epidemiology of head and neck cancer in Thailand. *Asia Pac J Clin Oncol*. 2018;14:16-22.
- Maier H, Dietz A, Gewelke U, Heller WD, Weidauer H. Tobacco and alcohol and the risk of head and neck cancer. *Clin Invest*. 1992;70:320-327.
- Chaturvedi AK, Engels EA, Pfeiffer RM, et al. Human papillomavirus and rising oropharyngeal cancer incidence in the United States. *J Clin Oncol*. 2011;29:4294-4301.
- Mehanna H, Beech T, Nicholson T, et al. Prevalence of human papillomavirus in oropharyngeal and nonoropharyngeal head and neck cancer—systematic review and meta-analysis of trends by time and region. *Head Neck*. 2013;35:747-755.
- Carlander A-L, Grønhøj Larsen C, Jensen DH, et al. Continuing rise in oropharyngeal cancer in a high HPV prevalence area: a Danish population-based study from 2011 to 2014. *Eur J Cancer*. 2017;70:75-82.
- Jiarpinitnun C, Larbcharoensub N, Pattaranutaporn P, et al. Characteristics and impact of HPV-associated p16 expression on head and neck squamous cell carcinoma in Thai patients. *Asian Pac J Cancer Prev*. 2020;21:1679-1687.
- Ang KK, Harris J, Wheeler R, et al. Human papillomavirus and survival of patients with oropharyngeal cancer. *N Engl J Med*. 2010;363:24-35.
- Pulte D, Brenner H. Changes in survival in head and neck cancers in the late 20th and early 21st century: a period analysis. *Oncologist*. 2010;15:994-1001.
- Chow LQM. Head and neck cancer. *N Engl J Med*. 2020;382:60-72.
- Kang H, Kiess A, Chung CH. Emerging biomarkers in head and neck cancer in the era of genomics. *Nat Rev Clin Oncol*. 2015;12:11-26.
- Nowicka Z, Stawiski K, Tomasik B, Fendler W. Extracellular miRNAs as biomarkers of head and neck cancer progression and metastasis. *Int J Mol Sci*. 2019;20:4799.
- Peng Y, Croce CM. The role of MicroRNAs in human cancer. *Signal Transduct Target Ther*. 2016;1:15004.
- Sannigrahi MK, Sharma R, Panda NK, Khullar M. Role of non-coding RNAs in head and neck squamous cell carcinoma: a narrative review. *Oral Dis*. 2018;24:1417-1427.
- Ela S, Mager I, Breakefield XO, Wood MJ. Extracellular vesicles: biology and emerging therapeutic opportunities. *Nat Rev Drug Discov*. 2013;12:347-357.
- Mathivanan S, Ji H, Simpson RJ. Exosomes: extracellular organelles important in intercellular communication. *J Proteomics*. 2010;73:1907-1920.
- Simpson RJ, Lim JW, Moritz RL, Mathivanan S. Exosomes: proteomic insights and diagnostic potential. *Expert Rev Proteomics*. 2009;6:267-283.

18. Liao J, Liu R, Shi YJ, Yin LH, Pu YP. Exosome-shuttling microRNA-21 promotes cell migration and invasion-targeting PDCD4 in esophageal cancer. *Int J Oncol*. 2016;48:2567-2579.
19. Salehi M, Sharifi M. Exosomal miRNAs as novel cancer biomarkers: challenges and opportunities. *J Cell Physiol*. 2018;233:6370-6380.
20. Mirzaei H, Sahebkar A, Jaafari MR, Goodarzi M, Mirzaei HR. Diagnostic and therapeutic potential of exosomes in cancer: the beginning of a new tale? *J Cell Physiol*. 2017;232:3251-3260.
21. Liao Y, Wang J, Jaehnig EJ, Shi Z, Zhang B. WebGestalt 2019: gene set analysis toolkit with revamped UIs and APIs. *Nucleic Acids Res*. 2019;47:W199-W205.
22. Pan CY, Lin WC. miR-TV: an interactive microRNA Target Viewer for microRNA and target gene expression interrogation for human cancer studies. *Database*. 2020;2020:baz148.
23. Théry C, Witwer KW, Aikawa E, et al. Minimal information for studies of extracellular vesicles 2018 (MISEV2018): a position statement of the International Society for Extracellular Vesicles and update of the MISEV2014 guidelines. *J Extracell Vesicles*. 2018;7:1535750.
24. Gupta A, Kumar R, Sahu V, et al. NFκB-p50 as a blood based protein marker for early diagnosis and prognosis of head and neck squamous cell carcinoma. *Biochem Biophys Res Commun*. 2015;467:248-253.
25. Liu Y, Tan YR, Sun WW, et al. Identification of SCARA5 as a potential biomarker for oral squamous cell carcinoma using MALDI-TOF-MS analysis. *Proteomics Clin Appl*. 2018;12:e1700180.
26. Weiland T, Eckert A, Tomazic PV, et al. DRH1 - a novel blood-based HPV tumour marker. *EBioMedicine*. 2020;56:102804.
27. Forner A, Reig M, Bruix J. Hepatocellular carcinoma. *Lancet*. 2018;391:1301-1314.
28. Wang J, Zhou Y, Lu J, et al. Combined detection of serum exosomal miR-21 and HOTAIR as diagnostic and prognostic biomarkers for laryngeal squamous cell carcinoma. *Med Oncol*. 2014;31:148.
29. Li L, Li C, Wang S, et al. Exosomes derived from hypoxic oral squamous cell carcinoma cells deliver miR-21 to normoxic cells to elicit a prometastatic phenotype. *Cancer Res*. 2016;76:1770-1780.
30. Gai C, Camussi F, Broccoletti R, et al. Salivary extracellular vesicle-associated miRNAs as potential biomarkers in oral squamous cell carcinoma. *BMC Cancer*. 2018;18:439.
31. Qin X, Guo H, Wang X, et al. Exosomal miR-196a derived from cancer-associated fibroblasts confers cisplatin resistance in head and neck cancer through targeting CDKN1B and ING5. *Genome Biol*. 2019;20:12.
32. Roman BR, Goldenberg D, Givi B. AHNS Series-Do you know your guidelines? Guideline recommended follow-up and surveillance of head and neck cancer survivors. *Head Neck*. 2016;38:168-174.
33. Guo R, Wang Y, Shi WY, Liu B, Hou SQ, Liu L. MicroRNA miR-491-5p targeting both TP53 and Bcl-XL induces cell apoptosis in SW1990 pancreatic cancer cells through mitochondria mediated pathway. *Molecules*. 2012;17:14733-14747.
34. Yan W, Zhang W, Sun L, et al. Identification of MMP-9 specific microRNA expression profile as potential targets of anti-invasion therapy in glioblastoma multiforme. *Brain Res*. 2011;1411:108-115.
35. Xiao Y, Hu F, Li M, et al. Interaction between linc01615 and miR-491-5p regulates the survival and metastasis of colorectal cancer cells. *Transl Cancer Res*. 2020;9:2638-2647.
36. Huang W-C, Chan S-H, Jang T-H, et al. miRNA-491-5p and GIT1 serve as modulators and biomarkers for oral squamous cell carcinoma invasion and metastasis. *Cancer Res*. 2014;74:751-764.
37. Bhagirath D, Yang TL, Bucay N, et al. microRNA-1246 is an exosomal biomarker for aggressive prostate cancer. *Cancer Res*. 2018;78:1833-1844.
38. Ostenfeld MS, Jeppesen DK, Laurberg JR, et al. Cellular disposal of miR23b by RAB27-dependent exosome release is linked to acquisition of metastatic properties. *Cancer Res*. 2014;74:5758-5771.
39. Hammoudeh S, Gadelhaq W, Janahi I. Prospective cohort studies in medical research. In: Barría RM, ed. *Cohort Studies in Health Sciences*. London, UK: IntechOpen Ltd; 2018:11-29.
40. Chung CH, Gillison ML. Human papillomavirus in head and neck cancer: its role in pathogenesis and clinical implications. *Clin Cancer Res*. 2009;15:6758-6762.
41. Nopmaneepaisarn T, Tangtaturonrasme N, Rawangban W, Vinayanuwattikun C, Keelawat S, Bychkov A. Low prevalence of p16-positive HPV-related head-neck cancers in Thailand: tertiary referral center experience. *BMC Cancer*. 2019;19:1050.
42. Arsa L, Siripoon T, Trachu N, et al. Discrepancy in p16 expression in patients with HPV-associated head and neck squamous cell carcinoma in Thailand: clinical characteristics and survival outcomes. *BMC Cancer*. 2021;21:504.

## SUPPORTING INFORMATION

Additional supporting information may be found online in the Supporting Information section.

**How to cite this article:** Panvongsa W, Siripoon T, Worakitchanon W, et al. Plasma extracellular vesicle microRNA-491-5p as diagnostic and prognostic marker for head and neck squamous cell carcinoma. *Cancer Sci*. 2021;112:4257-4269. <https://doi.org/10.1111/cas.15067>